View metadata, citation and similar papers at core.ac.uk
brought to you by CORE
provided by Institutional Repository of the Freie Universität Berlin

Mapping Minerals on Mars with CRISM: Atmospheric and Photometric Correction for MRDR Map Tiles, Version 2, and Comparison to OMEGA. P.C. McGuire[1,2,3,4,5,*], R.E. Arvidson[1], J.L. Bishop[6], A.J. Brown[6], S. Cull[1], R.O. Green[7], C. Gross[2], C.D. Hash[3,8], E. Hauber[9], D.C. Humm[3], R. Jaumann[9], L. Le Deit[9], E.R. Malaret[8], T.Z. Martin[7, retired], G.A.Marzo[10,11], M.F. Morgan[3], S.L. Murchie[3], J.F. Mustard[12], G. Neukum[2], M. Parente[15], T. Platz[2], T.L. Roush[11], F.P. Seelos[3], K.D. Seelos[3], M.D. Smith[13], M. Sowe[2], D. Tirsch[9], S. Walter[2], L. Wendt[2], S.M. Wiseman[1.12], and M.J. Wolff[14]. [1]Washington U., St. Louis, MO, [2]Freie U., Berlin, Germany, [3]JHU/APL, Laurel, MD, [4]U. Chicago, Chicago, IL, [5]West Virginia U., Morgantown, WV, [6]SETI, Mountain View, CA, [7]NASA/JPL, Pasadena, CA, [8]ACT, Reston, VA, [9]DLR, Berlin, Germany, [10]ENEA, C.R. Casaccia, Roma, Italy, [11]NASA/ARC, Moffett Field, CA, [12]Brown Univ., Providence, RI, [13]NASA/GSFC, Greenbelt, MD, [14]Space Sci.Inst., Milwaukee, WI; [*]Email: patrick.mcguire@mail.wvu.edu

Introduction: We assess a new version (version 2, v2) of photometric and atmospheric corrections applied to 72-band multispectral mapping data from the Compact Reconnaissance Imaging Spectrometer for Mars (CRISM) on the Mars Reconnaissance Orbiter (MRO). The corrections account for effects of varying observational conditions, including atmospheric CO_2 absorption, scattering by dust aerosols, and photometric geometry. We will discuss differences between versions of these corrections that are released and under development, and compare derived indicator maps for mafic, hydrated and/or sulfate, and phyllosilicate minerals covering the Nili Fossae and Libya Montes regions with similar indicator maps derived using data from the Observatoire pour la Minéralogie l'Eau, les Glaces et l'Activité (OMEGA) instrument on Mars Express.

The CRISM instrument acquires data in one of two modes, hyperspectral (FRT) or multispectral (MSP) [6]. Here we focus on CRISM's MSP operating mode. MSP images return 72 selected bands with the same spectral wavelength range and resolution as the FRT data. MSP data have ~200 m/pixel spatial sampling and image strips ~10 km wide and several hundred km long. Systematic multispectral imaging over the course of the mission has yielded $>10^5$ strips, which are assembled into 1,964 5x5 degree Multispectral Reduced Data Record (MRDR) tiles for global coverage.

Mineral indicator maps can be assembled from these data by calculating the strengths of characteristic absorption features in each pixel of the mapped data. These features occur at 1.9-2.5 μm in hydrated sulfate and phyllosilicate minerals, near 1 and/or 1.8-2.3 μm in mafic minerals such as olivine and pyroxene, near 1.5 and 2.0 μm in H_2O ice, and near 1.4, 2.0, and 2.2-2.3 μm in CO_2 ice. The indicators we use are "summary parameters" developed [8] for OMEGA and CRISM data.

The OMEGA instrument [1], a ~0.4-5 μm hyperspectral spectrometer, has been conducting similar orbital mapping of Mars though normally at spatial sampling >1000 m/pixel. CRISM's MRDR map tiles provide broad spatial coverage similar to OMEGA's, but at an improved spatial resolution.

Data Reduction: Version 1 (v1) of the CRISM MRDRs available from the Planetary Data System (PDS) were calculated from the $R/\pi\mathcal{F}_s$, where R is the radiance-on-sensor and $\mathcal{F}_s$ is the solar flux. Interpretability of surface mineralogy is improved by correcting for variable observing conditions [4]. V1 of these corrections assumes Lambertian scattering by the surface. Radiative transfer calculations to model observing conditions are pre-computed to create a multi-dimensional lookup table of corrections for each spectral band. This table models effects of scattering by different abundances of ice or dust aerosols, attenuation by atmospheric CO_2 (both estimated from climatological patterns [4]), and thermal emission (estimated from a physical thermal model). The v1 correction has been used to generate a global set of "Lambert albedo" MRDR map tiles that estimate surface reflectivity at a normal solar incidence angle in the absence of an atmosphere [3][4][6].

Corrections using v2 have recently been completed, and include several improvements: (a) attenuation by atmospheric CO_2 is scaled from the observed strength of the 2.0-μm CO_2 absorption for each pixel [5][9] instead of being estimated from climatology; (b) small changes in CRISM's wavelength calibration with temperature of the instrument optics are addressed [5][9]; and (c) the estimate of aerosol scattering is set to 0.30 for dust aerosols and 0.01 for ice aerosols (at MGS-TES reference wavelengths of 9.3 and 12.1 μm, respectively). Prototype 'v2' Lambert albedo MRDR map tiles include test areas in the Nili Fossae and Libya

Montes regions. Here we focus upon comparison of CRISM and OMEGA observations in Nili Fossae. A broad overview of the spectral contents of these prototype tiles is afforded by combining spectral summary parameters into thematic RGB composites, or "browse products," i.e., MAF for mafics and PHY for phyllosilicates.

We have found that by using fixed values for the aerosols instead of the MRO-based climatological values of the aerosols, that the frequency of overcorrected strips is reduced. The value of 0.30 for the dust-aerosol opacity is a typical value from the CRISM emission-phase-function dust climatology, and avoids the larger values of >0.60 which often overly correct for dust opacity. The value of 0.01 for the ice-aerosol opacity is also a typical value from the MRO/MARCI ice climatology, and avoids the larger values of >0.10 which overly correct for ice opacity. Furthermore, a value of 0.01 is chosen for the ice-aerosol opacity instead of 0.00, so that use of lookup tables will be with an interior, instead of a boundary, data point.

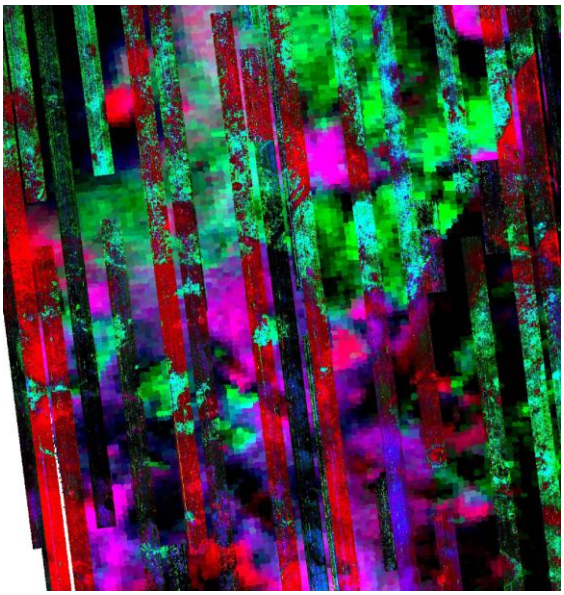

Figure 1: CRISM V2 MAF browse tile for MRDR#1249 at Nili Fossae overlain on OMEGA #424_4 MAF: r-OLINDEX, g-LCPINDEX, and b-HCPINDEX.

Results: Fig. 1 shows overlays (with an OMEGA MAF base map) of the CRISM MAF browse products of a single MRDR test tile in Nili Fossae to illustrate the current status of the v2 corrections. These maps are consistent in their mafic distributions, as mapped with hyperspectral CRISM and OMEGA data [7]. The CRISM high-calcium pyroxene index (HCPINDEX, blue) in the MAF map tile does not have the same range of values as in the OMEGA strip, but the olivine (OLINDEX, red) and low-calcium pyroxene (LCPINDEX, green) indicators appear to be similar. Comparisons of the olivine and pyroxene detections using CRISM MRDR strips and OMEGA cubes were similarly successful for the Libya Montes region and were included in a recent study [2]. Detections of Fe/Mg-rich phyllosilicates from the BD2290 indicator in the PHY map also compare well (not shown) with the detections indicated by BD2290 in OMEGA. However, parameters related to molecular water in minerals (BD1900, also not shown) can be systematically too high in the CRISM MRDR, perhaps due to incorrect estimation of the effects of ice aerosols. Generally, for this 'v2' tile and for other 'v2' tiles, correction for CO_2 absorption is much improved compared to the 'v1' tiles, allowing for cleaner detections of spectral structure in the 2-micron region, for example with BD1900.

Conclusion: The CRISM MRDR mapping tiles offer improved spatial resolution when compared to OMEGA mapping strips, and the mapped mineral distributions are similar in extent for both the CRISM MRDRs and OMEGA. The CRISM MRDR v2 map tiles have fewer outlying strips and fewer outlying spectra, when compared to the v1 map tiles. This improvement comes from using fixed ice and dust aerosol values, as well as, using the CRISM data itself to correct for CO_2 absorption at a wavelength of 2.0 μm.

References: [1] Bibring J.-P. et al. (2005) *Science* **307**, 1576–1581. [2] Bishop J. L. et al. (2013) JGR, in press. [3] Malaret E. et al. (2008) *LPSCXXXIX* #2081. [4] McGuire P.C. et al. (2008) *Trans. Geosci. Remote Sensing,* **46**(12) 4020-4040. [5] McGuire P.C. et al. (2009) *Planet. Space Sci.* **57**, 809-815. [6] Murchie S.L. et al. (2009) *JGR* **114**,E00D07. [7] Mustard J.F. et al. (2008) *Nature*, **454**, 305-309. [8] Pelkey S.M. et al. *JGR* **112**, E08S14. [9] Wiseman S.M. et al. (2010) *LPSCXLI*, #2461.